総　説

Heat Capacity of Nonstoichiometric Compounds

Hideaki Inaba and Keiji Naito*

Abstract

Difference in molar heat capacity due to nonstoichiometric composition is usually small as the Kopp-Neumann's law predicts, but it becomes large when the terms of heat capacity other than the classical harmonic vibrational term are prominent.

Origins of the deviation from the Kopp-Neumann's law come from all the terms of heat capacity: lattice heat capacity, heat capacity due to conduction electron, Schottky heat capacity, magnon heat capacity, heat capacity due to vacancy formation and heat capacity of phase transition.

Especially in the case when the phase transition occurs in nonstoichiometric compounds, the transition behavior depends sharply on nonstoichiometry. The transition temperature, enthalpy and entropy change for the transition as a function of nonstoichiometry obtained by the heat capacity measurement give important information on the mechanism of phase transition.

1. Contributions to heat capacity

Many information on solid state, such as lattice vibration, lattice expansion, electronic and magnetic state, lattice vacancy, phase transition etc. can be obtained from the heat capacity data.

The heat capacity at constant volume can be expressed as:

$$C_V = C_l + C_{e,c} + C_{e,s} + C_m + C_f + \cdots \qquad (1)$$

where C_l is the lattice heat capacity, $C_{e,c}$ the electronic heat capacity due to conduction electron, $C_{e,s}$ the electronic heat capacity due to electronic excitation to higher energy levels, C_m the magnon heat capacity due to the excitation of the spin system in magnetically ordered substances, C_f the heat capacity due to the formation of vacancies. Usually, the heat capacity at constant pressure, C_p, is measured and the relation between C_p and C_V is expressed as:

$$C_p = C_V + C_d \qquad (2)$$

$$C_d = \left(\frac{V\beta^2}{\kappa}\right) T = C_V \gamma \beta T \ , \qquad (3)$$

where β is the coefficient of cubical thermal expansion, κ the isothermal compressibility, V molar volume, γ Grüneisen constant ($\beta V/\kappa C_V$).

1.1 Lattice heat capacity

Since the phonon energy E_T is given by

$$E_T = \sum_{qj} \frac{\hbar\omega_{qj}}{\exp(\beta\hbar\omega_{qj})-1} \ , \qquad (4)$$

the lattice heat capacity is expressed as[1]:

$$C_V = \left(\frac{\partial E_T}{\partial T}\right)_V = k \sum_{qj} G(\beta\hbar\omega_{qj}) \ , \qquad (5)$$

where $G(x) = x^2 e^x/(e^x-1)^2$, ω vibrational frequency, k Boltzmann constant, $\beta = 1/kT$, q wave number, j branch.

The summation over q for each branch can be transformed into an integration over ω, using the density function $g_i(\omega)$. The expression (5) thus becomes

$$\begin{aligned} C_V &= k \sum_j \int G(\beta\hbar\omega) g_i(\omega) d\omega \\ &= k \int G(\beta\hbar\omega) g(\omega) d\omega \ , \end{aligned} \qquad (6)$$

where $g(\omega)$ is the sum of 3 branches of functions $g_i(\omega)$ and

$$g_i(\omega) = \frac{N\Omega}{8\pi^3} \iint \frac{dS}{|\mathrm{grad}_q \omega_{qj}|} \ , \qquad (7)$$

where N is the number of unit cell, Ω the volume of unit cell, dS is the elementary surface area, the vector $\mathrm{grad}_q \omega$ being perpendicular to the surface. $|\mathrm{grad}_q \omega_{qj}|$ is obtained from the dispersion relation between ω and q for each branch. The dispersion relation is usually obtained from the studies of the neutron inelastic scattering and infrared spectra. Dispersion relation and $g(\omega)$ of UO_2[2], K[3] and Al[4] have been obtained from the neutron inelastic scattering and those of PuO_2[5] and spinel[6] from the infrared spectra.

---

* Department of Nuclear Engineering, Faculty of Engineering, Nagoya University, Furo-cho, Nagoya, 464, Japan

In the Debye approximation the density function is

$$\left.\begin{aligned} g(\omega) &= \frac{9N\omega^2}{\omega_D}, \quad 0<\omega<\omega_D \\ &= 0, \quad \omega>\omega_D \end{aligned}\right\} \tag{8}$$

where ω_D is the Debye maximum frequency, and the Debye characteristic temperature θ is introduced as

$$k\theta = \hbar\omega_D \,. \tag{9}$$

The lattice heat capacity in the Debye approximation can be expressed as follows:

$$C_l = 9R\left(\frac{T}{\theta}\right)^3 \int_0^{\theta/T} \frac{e^x x^4}{(e^x-1)^2}\,dx = 3RD\left(\frac{\theta}{T}\right) , \tag{10}$$

where $D(\theta/T)$ is the tabulated Debye function, $x = T/\theta$. The equation (10) approaches to the Dulong-Petit value $3R$ above the Debye characteristic value θ.

The anharmonic term of lattice heat capacity, $C_{l,a}$ can not be described in the Debye approximation, but it is usually described as a term proportional to the temperature T[7,8]

$$C_{l,a} = \text{Const.}\ T \,. \tag{11}$$

1.2 Electronic heat capacity

The electronic heat capacity due to the conduction electron is given as follows[9]:

$$C_{e,c} = \gamma T\left[1-\left(\frac{3\pi^2}{10}\right)\left(\frac{T}{T_F}\right)^2\right] , \tag{12}$$

where γ is the electronic heat capacity coefficient, T_F Fermi temperature. Since usually $T \ll T_F$, the higher term can be ignored and $C_{e,c}$ is proportional to temperature.

The electronic heat capacity due to electronic excitation to higher energy levels, which is usually called as Schottky heat capacity, is described as follows[10,11]. The partition function Q is:

$$Q = \sum_{i=0}^{n} g_i \exp\left(-\frac{E_i}{RT}\right) . \tag{13}$$

When we put $E_0 = 0$, the average energy $\bar{E}$ is:

$$\bar{E} = Q^{-1} \sum_{i=1}^{n} g_i E_i \exp\left(-\frac{E_i}{RT}\right) . \tag{14}$$

Then,

$$\begin{aligned} C_{e,s} &= \left(\frac{\partial \bar{E}}{\partial T}\right) \\ &= Q^{-1} R^{-1} T^{-2} \left[Q_i \sum_{i=1}^{n} g_i E_i^2 \exp\left(-\frac{E_i}{RT}\right) \right. \\ &\quad \left. - \left\{ \sum_{i=1}^{n} g_i E_i \exp\left(-\frac{E_i}{RT}\right)\right\}^2 \right] \\ &= R^{-1} T^{-2} (\bar{E}^2 - (\bar{E})^2) . \end{aligned} \tag{15}$$

For two-level system $C_{e,s}$ is:

$$C_{e,s} = R\left(\frac{E_1}{RT}\right)^2 \left(\frac{g_1}{g_0}\right) \frac{\exp\left(-\frac{E_1}{RT}\right)}{\left\{1+\left(\frac{g_1}{g_0}\right)\exp\left(-\frac{E_1}{RT}\right)\right\}^2} . \tag{16}$$

where E_1 is the energy difference between the ground state and the first excited state.

$$\text{At} \quad T \ll \frac{E_1}{R} \quad C_{e,s} = R\left(\frac{g_1}{g_0}\right)\left(\frac{E_1}{RT}\right)\exp\left(-\frac{E_1}{RT}\right) . \tag{17}$$

$$\text{at} \quad T \gg \frac{E_1}{R} \quad C_{e,s} = R g_0 g_1 (g_0+g_1)^{-2} \left(\frac{E_1}{RT}\right)^2 . \tag{18}$$

1.3 Magnon heat capacity

The magnon heat capacity can be represented as follows[12]:

$$C_m^f = C^f R\left(\frac{RT}{2JS}\right)^{3/2} \quad \text{for ferromagnetics ,} \tag{19}$$

$$C_m = C^a R\left(\frac{RT}{2J'S}\right)^3 \quad \text{for antiferromagnetics ,} \tag{20}$$

where J and J' are exchange integrals, C^f and C^a constants depending on the type of crystal structure, and S is the spin.

1.4 Heat capacity due to the vacancy formation

Heat capacity due to the vacancy formation is given as[9]:

$$C_f = \left(\frac{\xi_f \Delta H_f^2}{RT^2}\right)\exp\left(\frac{-\Delta H_f}{RT}\right) . \tag{21}$$

where ξ_f is the entropy term of the vacancy formation, ΔH_f the vacancy formation energy.

2. Kopp-Neumann's law and heat capacity of nonstoichiometric compounds

According to the Dulong-Petit's law[13], as a three dimensional harmonic oscillator has an internal energy $3kT$ and a gram-atom of an element has N_A atoms, the heat capacity at constant volume is

$$\left(\frac{\partial E}{\partial T}\right)_V = C_V = 3N_A k = 3R. \tag{22}$$

The extension of Dulong-Petit's law was applied to chemical compounds, i.e., the molar heat capacity of a compound is equal to the sum of the atomic heat capacities of its constituent elements. This law which is generally referred to as the Kopp-Neumann's law[14] has been applied to predict the atomic heat capacity of alloys. If a compound consists of elements $1, 2, \cdots, n$ with atomic fraction $x_1, x_2, \cdots, x_n$, and atomic heat capacity $C_{p1}, C_{p2}, \cdots, C_{pn}$, then the heat capacity of the compound is

$$C_p = \sum_{i=1}^{n} x_i C_{pi} . \tag{23}$$

If equation (23) is applied to nonstoichiometric compounds, the difference in heat capacity among nonstoichiometric compounds is proportional to the difference in the composition, and it would be usually small compared with the experimental error of the heat capacity measurement.

Grønvold[15] measured heat capacities of $NiSe_{1-x}$ with different x-values and found that those per gram-atom at 800 K are nearly the same. Namba *et al.*[16] also found that heat capacities of $UC_{1-x}O_x$ were the same within experimental error between 300 to 700 K in spite of different x-values, although the heat of formation of $UC_{1-x}O_x$ varied with x. Heat capacities of Na_xWO_3[17] and Li_xWO_3[18] were measured by this authors and those per gram-atom at 700 and 800 K are given in Table 1, where we can see that they are equal within experimental error regardless of the difference of the composition, indicating that the Kopp-Neumann's law holds.

3. Deviations from the Kopp-Neumann's law in the nonstoichiometric compounds

If the Kopp-Neumann's law holds for nonstoichiometric compounds, we would have no longer reason to measure the heat capacities of nonstoichiometric compounds with different composition, because the heat capacity of nonstoichiometric compounds is determined by the atomic heat capacity and the atomic fraction of the constituents. However, the Kopp-Neumann's law is based on the Dulong-Petit's law and only the classical harmonic vibrational term of heat capacity is considered. Accordingly, in the nonstoichiometric compounds in which the terms other than the classical harmonic one are prominent, heat capacities of these compounds may deviate from the Kopp-Neumann's law. Origins of this deviation may come from all the terms of heat capacity as described in equation (1) as follows:

(a) Lattice heat capacity (b) Heat capacity due to conduction electron (c) Schottky heat capacity (d) Magnon heat capacity (e) Heat capacity due to the vacancy formation (f) Heat capacity due to phase transition. On the last term it will be described in the section 4.

3.1 Lattice heat capacity

Chernyaev *et al.*[19] measured heat capacities of VC_x with x-values of 0.460, 0.530, 0.712, 0.830 and 0.861 from 50 to 300 K and found heat capacities in these compounds largely deviated from the Kopp-Neumann's law in the low temperature and approached to the law at 300 K as shown in Fig. 1, where we can see that at low temperatures the deviation from the Kopp-Neumann's law is very large, but it becomes small at high temperatures. This shows that the bonding property of VC_x is dependent on the composition and the Debye characteristic temperature varies with x in carbide[20,21]. The difference in the Debye temperature results in large difference in heat capacity at low temperatures, but small difference in heat capacity at high

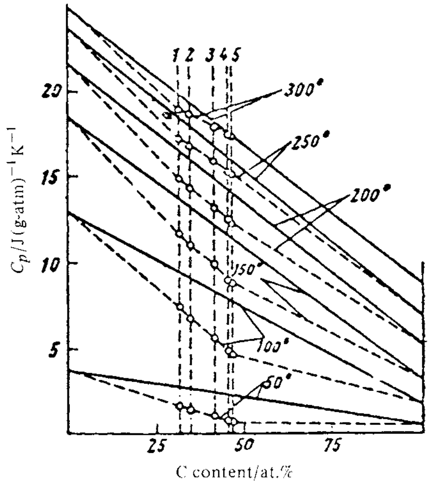

Fig. 1 Composition dependence on heat capacity of VC_x, x: 1-0.460, 2-0.530, 3-0.712, 4-0.830, 5-0.861 as a function of temperature. The solid line shows the Kopp-Neumann's law.[19]

Table 1 Heat capacity of Li_xWO_3 and Na_xWO_3 per gram-atom ($1/(4+x)$ mol)[17,18]

T/K	C_p/J mol^{-1}K^{-1}					
	$Li_{0.363}WO_3$	$Li_{0.478}WO_3$	$Li_{0.478}WO_3$	$Na_{0.485}WO_3$	$Na_{0.698}WO_3$	$Na_{0.794}WO_3$
700	25.34	25.33	25.97	25.06	25.03	25.07
800	25.74	25.96	26.62	25.69	25.52	26.62

temperatures.

It has been found that the Debye temperature varies with composition of nonstoichiometric compounds, such as TaC_x 20), NbC_x 22,23), PdH_x 23), NbO_x and TiO_x 24), NiS_x 25), NiH_x 26) and $Ni_xFe_{3-x}O_4$ 27).

3.2 Heat capacity due to conduction electron

The electronic heat capacity coefficient in nonstoichiometric compounds varies with the composition, resulting from the different band structure depending on the composition. The electronic heat capacity coefficient of Na_xWO_3 28) with x values of 0.56, 0.65, 0.73, 0.81 and 0.89 was measured and the density of states at the Fermi surface was obtained as a function of x, deviating from the free-electron approximation.

The electronic heat capacity coefficient has been measured in nonstoichiometric compound with different composition, such as VC_x 20), TaC_x 20), PdH_x 23), NbO_x 24), NiS_x 25), NiH_x 26), TiO_x 24) and $V_{3\pm x}Si$ 29).

3.3 Schottky heat capacity

The difference in the composition results in the difference in the valence of the magnetic ion and that in the crystal field around the magnetic ion. Accordingly, the Schottky heat capacity may vary with the composition in the nonstoichiometric compounds. Mitarov *et al.* 30) obtained Schottky heat capacity of $PrTe_x$ with x-values of 1.33, 1.37, 1.47 and 1.50 by measuring the heat capacities of $PrTe_x$ and $LaTe_x$ with the same x-values in the temperature range from 5 to 273 K. The Schottky term of the heat capacity of $PrTe_x$ was obtained by subtracting the heat capacity of $LaTe_x$ with the same x-value from that of $PrTe_x$. From the Schottky heat capacity thus determined, the energy levels splitted from the ground state $4f^2(^3H_4)$ of Pr^{3+} ion by the crystal field were obtained with different x-values and were compared with the calculated values, resulting in good agreement except for the higher energy levels.

A prominent Schottky effect is seen in US_2 and $US_{1.9}$ 31,32), where heat capacity of $US_{1.9}$ is larger than that of US_2 as seen in Fig. 2a. This is interpreted to mean that the energy difference ($\Delta E/k$) between the ground state and the excited state is 56 K for four-fifth U atoms and 68 K for one-fifth U atoms in the case of $US_{1.9}$, as shown in Fig. 2b, while it is the larger value, 144 K, in the case of US_2.

Schottky heat capacity as a function of composition was also measured in $Mn_xFe_{3-x}O_4$ 33).

3.4 Magnon heat capacity

Varazashvili *et al.* 34) observed that the heat capacities of $Ni_{1-x}Zn_xFe_2O_4$ at the room temperature were dependent on x-values and showed a maximum around $x = 0.4$. This behavior comes from the magnetic origin, since the saturated magnetization is also dependent on x-values and its maximum is around $x = 0.4$.

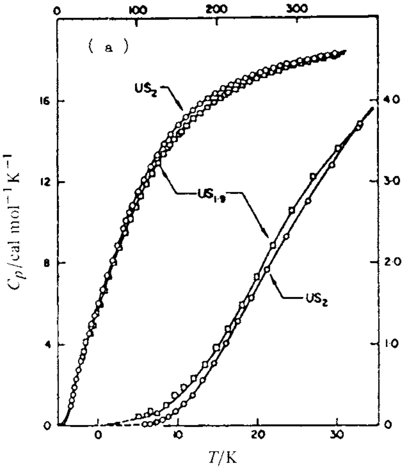

Fig. 2a Comparison of heat capacities of US_2 and $US_{1.9}$

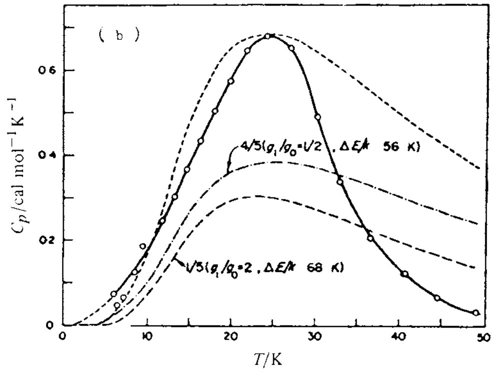

Fig. 2b Resolution of the excess heat capacity of $US_{1.9}$. The contribution of the atoms with $\Delta E/k$ = 68 K is shown by — — —, that of the other four-fifths by —·—·—and the sum by - - - - . The circles and the solid line represent the excess heat capacity obtained by subtracting a lattice contribution estimated by fitting the observed heat capacity at higher temperatures to a suitable Debye function from the observed heat capacity.31,32)

The heat capacity and magnetic susceptibility of $UC_{1-x}N_x$ with different x-values were measured by Novion and Costa35,36). The magnetic susceptibility of $UC_{1-x}N_x$ was changed with x-values. The lattice and electronic heat capacity are obtained from the C_p/T against T^2 plot, but the magnon heat capacity was not separated, perhaps because the heat capacity for antiferromagnetics is a function of T^3, being the same temperature dependence of lattice heat capacity.

3.5 Heat capacity due to the vacancy formation

Affortit and Marcon[37] measured heat capacities of $(U_{0.8}Pu_{0.2})O_x$ with x-values of 1.98, 2.00, 2.045 and 2.08 in the temperature range from 1500 to 3000 K, and their results are shown in Fig. 3. The differences in the heat capacities increased with temperature, and they are 4–16% at 2500 K, largely deviated from the Kopp-Neumann's law. This difference in heat capacity may come from the difference in the concentration of the interstitial and vacancy sites and the difference in the activation energy of the vacancy formation.

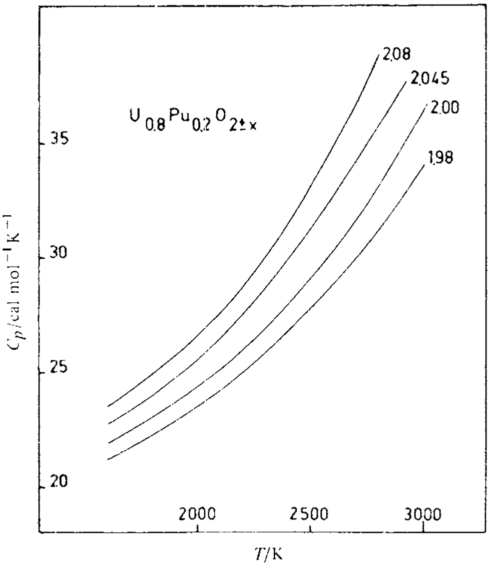

Fig. 3 Heat capacities of $UO_{0.8}Pu_{0.2}O_{2\pm x}$ as a function of T.[37]

Turchanin *et al.*[38] measured heat capacities of VC_x with x-values of 0.72, 0.75 and 0.86 in the temperature range from 1300 to 2500 K and found that the heat capacities per gram-atom varied with the composition of the carbides. This dependence of the heat capacity on the composition was ascribed to the fact that the metal-metal bond energy changed with increased defect state of the C-sublattice. Similar studies were made in NbC_x[39], ZrC_x[40] and TaC_x[40].

4. Heat capacity due to phase transition in nonstoichiometric compounds

As was seen in the previous section, the difference in nonstoichiometric composition results in the difference in the properties of the compound such as the bonding nature, the valence state of cation and vacancy concentration. When phase transition occurs in nonstoichiometric compounds, such difference in the properties depending on nonstoichiometry may be largely revealed, and the transition behavior, such as transition temperature, enthalpy and entropy change for the transition depend strongly on nonstoichiometry. Accordingly, if we obtain these quantities as a function of nonstoichiometry by the heat capacity measurement, they will give important information on the mechanism of the phase transition.

Heat capacities due to several types of phase transition have been measured as a function of nonstoichiometry as follows:

(a) Order-disorder transition of atomic configuration
(b) Magnetic transition (c) Superconducting transition
(d) Semimetal-metal transition (e) Order-disorder transition due to valence electron.

4.1 Order-disorder transition of atomic configuration

The theory of the order-disorder transition has been developed in binary alloys. The method of Bragg and Williams[41,42] is a simple, yet successful, approximate method. The result of the Bragg-Williams approximation is as follows. The heat capacity and entropy change for the order-disorder of a binary alloy is described in terms of the long-range order parameter s:

$$C = \frac{RT_c^2\{1-\tanh(\frac{2T_c s}{T})\}}{T^2-TT_c\{1-\tanh(\frac{2T_c s}{T})\}} \qquad (24)$$

$$g(s) = \left\{\frac{\frac{N}{2}!}{\frac{N}{4}(1+s)!\,\frac{N}{4}(1-s)!}\right\}^2, \qquad (25)$$

and

$$\Delta S = k\ln\{g(s_2)\} - k\ln\{g(s_1)\} \quad . \qquad (26)$$

where C is heat capacity due to the order-disorder rearrangement, T_c the critical temperature, $g(s)$ the number of possible ways of rearranging atoms, ΔS the entropy change from s_2 to s_1 and it becomes $R\ln 2$, when the transition occurs from completely ordered to completely disordered state.

The order-disorder transition was found in nonstoichiometric TiO_x and the heat capacities of TiO_x with x-values from 0.08 to 0.40 were measured by Koiwa and Hirabayashi[43]. The enthalpy and entropy change for the transition against O/Ti ratio is shown in Fig. 4. This transition has been interpreted as mainly

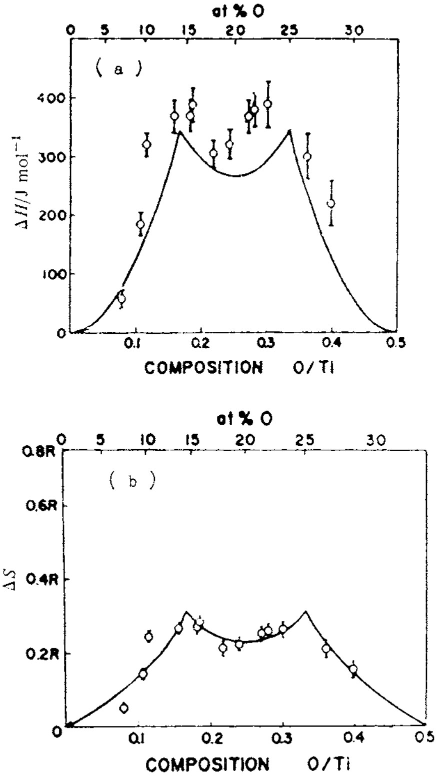

Fig. 4 Composition dependence of enthalpy change (a) and entropy change (b) for the transition. Solid lines show the theoretical curves for the intra-plane disordering.[43,45]

the intra-plane disordering of interstitial oxygen atoms dissolved in the h.c.p. lattice of α-Ti[44,45] and the enthalpy and entropy change for the transition were calculated[45] by the Bragg-Williams approximation as shown in Fig. 4 in relatively good agreement with the observed values.

Heat capacities of $Ni_{1-x}Se$ phase with different x-values have been measured by Grønvold *et al.*[15,46] λ-type transitions were observed in all $Ni_{1-x}Se$ samples ($1-x=0.925$, 0.90, 0.889, 0.861, 0.85, 0.8375, 0.825, 0.8125, 0.775 and 0.75) due to vacancy disordering in the NiAs-like structures. The entropy change of the disordering was calculated as a first approximation as:

$$\Delta S = -\frac{R}{2}\{(1-x)\ln(1-x)+x\ln x\}. \qquad (27)$$

Similar heat capacity measurement has been made by Grønvold *et al.* in nonstoichiometric compounds such as $Fe_{1-x}Se$[47] and $Ni_{3\pm x}Te$[48].

4.2 Magnetic transition

R. Mainard *et al.* measured heat capacity anomalies of Fe_xO, with x-values of 0.944, 0.937, 0.927, 0.923 and 0.899[49]. The peak maximum in the heat capacity curve decreases linearly with increasing x, confirming the variation of Neel temperature with x derived from magnetic susceptibility measurements by Koch and Fine[50].

Heat capacity measurement on US_xP_{1-x} with x-values of 0.75, 0.50, 0.25 was reported by Counsell *et al.*[51]. US and UP are known as ferromagnetic and antiferromagnetic respectively, but ferromagnetic interactions predominate over antiferromagnetic interactions in US_xP_{1-x}. As P is progressively substituted for S in US, the magnetic ordering temperature decreases and the entropy increment becomes smaller. Recently, heat capacity of US_xP_{1-x} with ten x-values has been measured by Yokokawa *et al.*[52]. The magnetic ordering temperature, the peak maximum of heat capacity and other thermodynamic parameters have been obtained against the composition.

Heat capacity of $Mn_xFe_{3-x}O_4$ with different x-values has been measured by this authors[53] and the entropy change due to the transition was discussed as a function of the composition. The entropy change is mainly due to magnetic origin, but some extra contributions to the entropy change are considered.

Heat capacities of $Fe_{1-x}Co_xS_2$ and $Co_{1-x}Ni_xS_2$ were measured by Ogawa[54] and the magnetic entropy, density of states and the Debye temperature of these compounds were discussed as a function of x.

4.3 Superconducting transition

Heat capacities of NbC_x and TaC_x with different x-values have been measured by Toth *et al.*[20]. The superconducting critical temperature T_c decreases with decrease of x in the carbides as shown in Fig. 5. The Debye temperature Θ, electronic heat capacity coefficient γ and superconducting parameters $N(0)$ and V_{ph} are also decreases with decrease of x.

Zimmermann *et al.*[23] found from the heat capacity measurement of PdH_x that T_c, Θ and γ varied with x. Similar study on superconducting transition has been made in the nonstoichiometric compounds such as NbO_x, TiO_x[24] and $V_{3-x}Si$[29] by the heat capacity measurement.

4.4 Semimetal-metal transition

Heat capacity measurement has been made by Coey and Brusetti[25] from 5 to 330 K on Ni_xS with x-values of 0.95, 0.98 and 1.00. As shown in Fig. 6, a sharp maximum of heat capacity in $Ni_{1.00}S$ was obtained at 265 K, indicating a semimetal (low temperature phase) to metal (high temperature phase) phase transition of

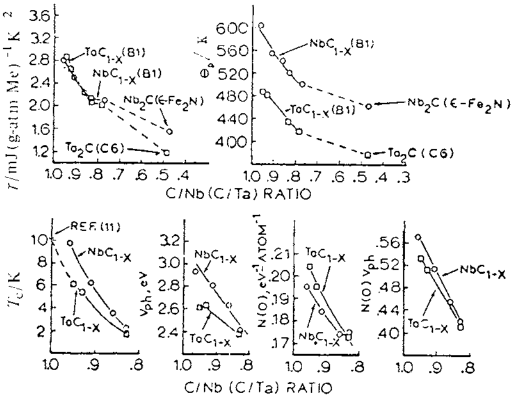

Fig. 5 Variation of the thermodynamic and superconducting properties with C/Nb and C/Ta ratio.[20)]

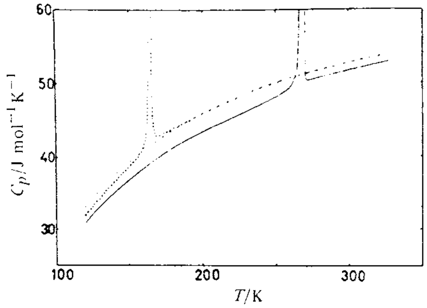

Fig. 6 Heat capacity as a function of temperature for: Solid line, $Ni_{1.00}S$; dotted line, $Ni_{0.98}S$; dashed line, $Ni_{0.95}S$.[25)]

Table 2 Changes in thermodynamic parameters at the first-order transition in nickel sulfide.[25)]

Sample	T_t/K	ΔH/J mol^{-1}	ΔS/J mol^{-1}K^{-1}	ΔC_p/J mol^{-1}K^{-1}
$Ni_{1.00}S$	265	1409±42	5.32±0.16	0.8±0.5
$Ni_{0.98}S$	165	454±14	2.80±0.09	1.0±0.5
$Ni_{0.95}S$	< 4.2	——	——	——

first order. In $Ni_{0.98}S$ the transition temperature shifted to 165 K, and in $Ni_{0.95}S$ the phase transition was not observed. Changes in thermodynamic parameters at first order transition in nickel sulfide are given in Table 2. The electronic heat capacity coefficient and the Debye temperature of these compounds were also largely dependent on nonstoichiometry. The entropy change for the transition was resolved into electronic, vibrational and magnetic contributions.

4.5 Order-disorder transition of valence electron

Heat capacity of nonstoichiometric U_4O_{9-y} was measured by Inaba and Naito[55)] with different y-values and the transition temperature, enthalpy and entropy changes for the transition were obtained as a function of y. This phase transition is thought to be originated from an order-disorder rearrangement of U^{4+} and U^{5+} ions and succeeding displacement of oxygen ions. The entropy change as a function of y is elucidated as follows[55,56)]. The entropy change ΔS is the sum of that due to the displacement of oxygen ions, ΔS_d, and that due to the order-disorder rearrangement of U^{4+} and U^{5+} ions, ΔS_e:

$$\Delta S = \Delta S_d + \Delta S_e \quad . \tag{28}$$

As for ΔS_d, it is calculated from the numbers of oxygen atoms of normal fluorite sites and interstitial sites in the low- and high-temperature phases, which are obtained from X-ray diffraction data[57)] of superlattice lines, based on the Willis model. The results are given in Table 3.

As for ΔS_e, it is estimated from the jump width of electrical conductivity. Electrical conduction in U_4O_{9-y} is believed to occur via a hopping mechanism, and the Z-type jump of electrical conductivity is originated from the increment of the probability for hopping between U^{4+} and U^{5+} ions. ΔS_e is thought to correspond to this increment of probability for hopping and also correspond to the vibrational entropy change, namely

$$\Delta S_e \propto \log\frac{\nu_h}{\nu_l} - J \quad , \tag{29}$$

where ν_h and ν_l are the hopping frequency in the high- and low-temperature phase, and J is the jump width of electrical conductivity. One can therefore calculate the variation of ΔS_e among samples with different O/U ratios from the jump width of electrical conductivity. As seen in Table 3, since the entropy change due to the displacement of oxygen ions ΔS_d is zero in the case of $UO_{2.250}$, the observed entropy change 1.92 J mol^{-1}K^{-1} is thought to represent ΔS_e. Therefore, ΔS_e for sub-stoichiometric samples can be calculated using equation (29) and the results are given in Table 4. The total entropy change ($\Delta S_e + \Delta S_d$) thus calculated and the observed entropy change are given in Table 4, from which we can see that the calculated values are in fairly

Table 3 The compositions of U_4O_{9-y} in the low- and high-temperature phases: I_h and I_l represent the intensity of superlattice lines of U_4O_{9-y} in the high- and low-temperature phases, respectively. ΔS_n is the entropy change due to the normal fluorite sites and ΔS_i is that due to the displacement in the interstitial sites.[55)]

	I_h/I_l	Composition of low-temperature phase	Composition of high-temperature phase	$\frac{\Delta S_n}{\mathrm{J\ mol^{-1}\ K^{-1}}}$	$\frac{\Delta S_i}{\mathrm{J\ mol^{-1}\ K^{-1}}}$	$\frac{\Delta S_d}{\mathrm{J\ mol^{-1}\ K^{-1}}}$
$UO_{2.230}$	2.0	$UO_{2-0.096}O'_{0.163}O''_{0.163}$	$UO_{2-0.230}O'_{0.230}O''_{0.230}$	2.72	−0.75	1.97
$UO_{2.240}$	1.55	$UO_{2-0.146}O'_{0.193}O''_{0.193}$	$UO_{2-0.240}O'_{0.240}O''_{0.240}$	1.76	−0.75	1.01
$UO_{2.250}$	1.0	$UO_{2-0.250}O'_{0.250}O''_{0.250}$	$UO_{2-0.250}O'_{0.250}O''_{0.250}$	0	0	0

Table 4 Relative jump width and entropy change calculated and observed for the transition for U_4O_{9-y} samples.[56)]

	relative jump width	$\frac{\Delta S_e}{\mathrm{J\ mol^{-1}\ K^{-1}}}$	$\frac{\Delta S_d}{\mathrm{J\ mol^{-1}\ K^{-1}}}$	calculated entropy change $\frac{\Delta(S_e+S_d)}{\mathrm{J\ mol^{-1}\ K^{-1}}}$	observed entropy change $\frac{\Delta S}{\mathrm{J\ mol^{-1}\ K^{-1}}}$
$UO_{2.250}$	1.0	1.92	0.0	1.92	1.92
$UO_{2.240}$	0.68	1.30	1.00	2.30	2.34
$UO_{2.228}$	0.60	1.17	2.01*	3.18	2.93

* It is calculated on the basis of the assumption that the ratio I_h/I_l is 2.0, which is the same value as for $UO_{2.230}$.

good agreement with the observed ones.

4.6 Other examples

Heat capacity of Na_xWO_3 with x-values of 0.485, 0.698 and 0.794 was measured by this authors[17)] and a λ-type heat capacity anomaly was observed around 400 K, as shown in Fig. 7. The entropy change due to the transition was obtained as a function of x. It is supposed that the entropy change due to the transition is caused by the increase in the number of slightly displaced atoms with respect to the ideal perovskite position. Similar λ-type heat capacity anomalies were observed in Li_xWO_3 with x-values of 0.363, 0.437 and 0.478[18)].

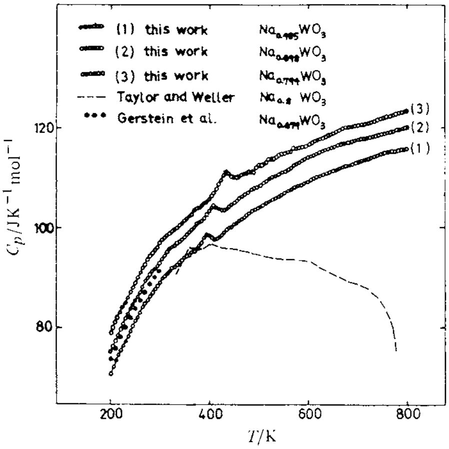

Fig. 7 Heat capacities of $Na_{0.485}WO_3$, $Na_{0.698}WO_3$ and $Na_{0.794}WO_3$ with results of $Na_{0.679}WO_3$ by Gerstein *et al.* and those of $Na_{0.8}WO_3$ by Taylor and Weller.[17)]

References

1) B. Donovan and J. F. Angress, "Lattice Vibrations" Chapman and Hall Ltd. (1970)
2) G. Dolling, R.A. Cowley and A.D.B. Woods, *Can. J. Phys.* 43 1397 (1965)
3) R.A. Cowley, *Phys. Rev.* 150 487 (1966)
4) G. Gilat, *Phys. Rev.* 143 487 (1966)
5) L. Manes, "Plutonium 1970 and other Actinides" Part 1 P. 254
6) N.W. Grimes, *Spectrochim. Acta.* 28A 2217 (1972)
7) R. E. Peierls, "Quantum Theory of Solids" The Oxford University Press (1955)
8) C. R. Brooks, *J. Phys. Chem. Solids* 29 1377 (1968)
9) A. H. Wilson, "The Theory of Metals" 2nd Edn. P. 144 Cambridge
10) B. Justice and E. F. Westrum, *J. Phys. Chem.* 67 339 (1963)
11) I. A. Smirnov, *Phys. Status Solidi* 14 363 (1972)
12) E. S. R. Gospel, "Specific Heats at low Temperatures" Plenum Press (1966)

13) P. L. Dulong and A. T. Petit, *Ann. Chim.* 10 395 (1819)
14) F. Seitz, "The Modern Theory of Solids" McGraw-Hill Book Co. Inc. P. 38 (1940)
15) F. Grϕnvold, *Acta Chem. Scand.* 21 1036 (1970)
16) S. Namba, S. Imoto and T. Sano, *Nippon Genshiryoku Gakkaishi* 9 2 (1967)
17) H. Inaba and K. Naito, *J. Solid State Chem.* 15 283 (1975)
18) H. Inaba and K. Naito, *J. Solid State Chem.* 18 279 (1976)
19) V. S. Chernyaev, E. N. Zhetnikov, G. P. Shveikin, R. P. Krenzhis and P. V. Gelid, *Isv. Akad. Nauk SSSR Neorg. Mater.* 3 789 (1967)
20) L. E. Toth, M. Ishikawa and Y. A. Chang, *Acta Metall.* 16 1183 (1968)
21) V. A. Zkxai, V. S. Mokronosov, V. S. Chernyaev and P. V. Gelid, *Zh. Neorg. Khim.* 16 611 (1971)
22) T. K. Sandenaw and E. K. Storms, *U S. At. Energy Comms* LA-3331 (1965)
23) M. Zimmermann, G. Wolf and K. Bohmhammel, *Phys. Status Solidi,* A 31 511 (1975)
24) A. M. Okaz and P. H. Keesom, *Phys. Rev.* B 12 4917 (1975)
25) J. M. D. Coey and R. Brusetti, *Phys. Rev.* B 11 671 (1975)
26) G. Barkleit and G. Worf, *Phys. Status Solidi* 28 139 (1975)
27) S. R. Pollack and K. R. Atkins, *Phys. Rev.* 125 1248 (1962)
28) R. W. Vest, M. Griffel and J. F. Smith, *J. Chem. Phys.* 28 293 (1958)
29) J. Bonnerot, J. Hallais, S. Barisic and J. Labbe, *J. Phys. (Paris)* 30 701 (1969)
30) R.G. Mitarov, V.V. Tikhonov, L.N. Vasilev, A.V. Golubkov and I.A. Smirnov, *Phys. Status Solidi* A 30 457 (1975)
31) F. Grϕnvold and E. F. Westrum, *J. Inorg. Nucl. Chem.* 30 2127 (1968)
32) E. F. Westrum and F. Grϕnvold, *J. Inorg. Nucl. Chem.* 32 2169 (1970)
33) B. Low, *J. Appl. Phys.* 34 1250 (1963)
34) V.S. Varazashvili, N.A. Landiya, G.D. Chachanidge and N.G. Ledgava, *Isv. Akad. Nauk SSSR Neorg. Mater.* 4 1160 (1968)
35) C.-H. Novion and P. Costa, *C.R. Acad. Sci. Paris* 270 1415 (1970)
36) C.-H. Novion and P. Costa, *J. Phys. (Paris)* 33 257 (1972)
37) C. Affortit and J.-P. Marcon, *Rev. Int. Hautes. Temp. Ref.* 7 236 (1970)
38) A. G. Turchanin, E. A. Gusheva, V. V. Morozov, A. S. Bolgar and V. V. Feshenko, *Isv. Akad. Nauk SSSR Neorg. Mater.* 10 1619 (1974)
39) A. G. Turchanin, *Tr. Nauch. Konf. Aspir. Inst. Probl. Materialoved Akad. Ukr. SSR.* Ist 1967 (Pub. 1968) P. 88–99
40) I. G. Korshunov and V. S. Chernyaev, *Tr. Ural. Politekh. Inst.* 231 164 (1974)
41) W. L. Bragg and E. J. Williams, *Proc. Roy. Soc.* A145 699 (1934)
42) W. L. Bragg and E. J. Williams, *Proc. Roy. Soc.* A151 540 (1935)
43) M. Koiwa and M. Hirabayashi, *J. Phys. Soc. Jpn.* 27 801 (1969)
44) S. Yamaguchi, *J. Phys. Soc. Jpn.* 27 155 (1969)
45) M. Koiwa and M. Hirabayashi, *J. Phys. Soc. Jpn.* 27 807 (1969)
46) F. Grϕnvold, N. J. Kveseth and A. Sveen, *J. Chem. Thermodyn.* 7 617 (1975)
47) F. Grϕnvold, *Acta Chem. Scand.* 22 1219 (1968)
48) F. Grϕnvold, N. J. Kveseth and A. Sveen, *J. Chem. Thermodyn.* 4 337 (1972)
49) R. Mainard, M. Boubel and H. Fousse, *C.R. Acan. Sci. Paris* 266B 1299 (1968)
50) F. B. Koch and M. E. Fine, *J. Appl. Phys.* 38 1470 (1967)
51) J. F. Cousell, J. F. Martin, R. M. Dell and A. R. Junkison, "Thermodynamics of Nuclear Materials 1962" IAEA Vienna P. 385
52) H. Yokokawa, Y. Takahashi and T. Mukaibo, Oral presentation at the 12th Meeting of Discussions on Calorimetry and Thermal Analysis in Japan, Lecture No. 1205 (1976)
53) K. Naito, H. Inaba and H. Yagi, unpublished data
54) S. Ogawa, *J. Phys. Soc. Jpn.* 41 462 (1976)
55) H. Inaba and K. Naito, *J. Nucl. Mater.* 49 181 (1973/74)
56) H. Inaba, T. Matsui and K. Naito, *J. Nucl. Mater.* 58 115 (1975)
57) T. Ishii, K. Naito, K. Oshima and Y. Hamaguchi, *J. Phys. Chem. Solids* 32 235 (1971)

要　　旨

コップーノイマンの法則が示すように，不定比組成の違いによる熱容量の差は，通常小さいが，古典的な調和振動項以外の寄与が顕著となる時は，その差が大きくなる。

コップーノイマンの法則から外れる原因は，熱容量の全ての項から成る。即ち，格子熱容量，伝導電子熱容量，ショットキー熱容量，磁気熱容量，格子欠陥生成熱容量そして相転移熱容量である。

特に不定比化合物において，相転移がある場合には，不定比組成の関数として，転移温度，転移のエンタルピー，エントロピー変化が熱容量測定から得られると，それらは，相転移機構に関して重要な知見を与える。